Physics Letters B 755 (2016) 92–96

Contents lists available at ScienceDirect

Physics Letters B

www.elsevier.com/locate/physletb

Measurement of the absolute differential cross section of proton–proton elastic scattering at small angles

D. Mchedlishvili [a,b], D. Chiladze [a,b], S. Dymov [c,b], Z. Bagdasarian [a,b], S. Barsov [d], R. Gebel [b], B. Gou [e,b], M. Hartmann [b], A. Kacharava [b], I. Keshelashvili [b], A. Khoukaz [f], P. Kulessa [g], A. Kulikov [c], A. Lehrach [b], N. Lomidze [a], B. Lorentz [b], R. Maier [b], G. Macharashvili [a,c], S. Merzliakov [c,b], S. Mikirtychyants [b,d], M. Nioradze [a], H. Ohm [b], D. Prasuhn [b], F. Rathmann [b], V. Serdyuk [b], D. Schroer [f], V. Shmakova [c], R. Stassen [b], H.J. Stein [b], H. Stockhorst [b], I.I. Strakovsky [h], H. Ströher [b], M. Tabidze [a], A. Täschner [f], S. Trusov [i,j], D. Tsirkov [c], Yu. Uzikov [c], Yu. Valdau [d,k], C. Wilkin [l,*], R.L. Workman [h], P. Wüstner [m]

[a] High Energy Physics Institute, Tbilisi State University, GE-0186 Tbilisi, Georgia
[b] Institut für Kernphysik, Forschungszentrum Jülich, D-52425 Jülich, Germany
[c] Laboratory of Nuclear Problems, JINR, RU-141980 Dubna, Russia
[d] High Energy Physics Department, Petersburg Nuclear Physics Institute, RU-188350 Gatchina, Russia
[e] Institute of Modern Physics, Chinese Academy of Sciences, Lanzhou 730000, China
[f] Institut für Kernphysik, Universität Münster, D-48149 Münster, Germany
[g] H. Niewodniczański Institute of Nuclear Physics PAN, PL-31342 Kraków, Poland
[h] Data Analysis Center at the Institute for Nuclear Studies, Department of Physics, The George Washington University, Washington, D.C. 20052, USA
[i] Institut für Kern- und Hadronenphysik, Forschungszentrum Rossendorf, D-01314 Dresden, Germany
[j] Department of Physics, M.V. Lomonosov Moscow State University, RU-119991 Moscow, Russia
[k] Helmholtz-Institut für Strahlen- und Kernphysik, Universität Bonn, D-53115 Bonn, Germany
[l] Physics and Astronomy Department, UCL, London WC1E 6BT, UK
[m] Zentralinstitut für Engineering, Elektronik und Analytik, Forschungszentrum Jülich, D-52425 Jülich, Germany

ARTICLE INFO

Article history:
Received 21 October 2015
Received in revised form 30 January 2016
Accepted 31 January 2016
Available online 3 February 2016
Editor: V. Metag

Keywords:
Proton–proton elastic scattering
Differential cross section

ABSTRACT

The differential cross section for proton–proton elastic scattering has been measured at a beam kinetic energy of 1.0 GeV and in 200 MeV steps from 1.6 to 2.8 GeV for centre-of-mass angles in the range from 12°–16° to 25°–30°, depending on the energy. A precision in the overall normalisation of typically 3% was achieved by studying the energy losses of the circulating beam of the COSY storage ring as it passed repeatedly through the windowless hydrogen target of the ANKE magnetic spectrometer. It is shown that the data have a significant impact upon the results of a partial wave analysis. After extrapolating the differential cross sections to the forward direction, the results are broadly compatible with the predictions of forward dispersion relations.

For beam energies above about 1 GeV there are relatively few measurements of proton–proton elastic scattering at centre-of-mass (c.m.) angles θ from 10° to 30°, i.e., between the region of major Coulomb effects and the larger angles where the EDDA Collaboration has contributed so extensively [1–3]. The lack of information on the differential cross section and analysing power inevitably leads to ambiguities in any *pp* partial wave analysis (PWA) at high energies [4]. The ANKE Collaboration has recently published proton analysing powers in this angular domain at 796 MeV and five other beam energies between 1.6 and 2.4 GeV using a polarised proton beam [5] and these led to a revision of the SAID PWA [4] in order to accommodate the data. The major uncertainty in such a measurement is the precision to which the beam polarisation can be determined, beam-target luminosity and equipment acceptance playing only secondary roles. This is far from being the case for the differential cross section where, in order to provide accurate absolute values, both the luminosity and acceptance must be mastered with high precision [6]. The difficulties encountered

* Corresponding author.
E-mail address: c.wilkin@ucl.ac.uk (C. Wilkin).

http://dx.doi.org/10.1016/j.physletb.2016.01.066

in earlier experiments in making absolute measurements were discussed most clearly in Ref. [7], whose normalisation was used as the standard for the EDDA work [1,2].

As was the case for the analysing power [5], the present studies of the differential cross section were carried out using the ANKE magnetic spectrometer [8] sited inside the storage ring of the COoler SYnchrotron (COSY) [9] of the Forschungszentrum Jülich. Only the Forward Detector (FD), which measured fast protons from elastic pp scattering over a range of up to 12°–30° in c.m. polar angles and ±30° in azimuth, was used in the analysis. The FD comprises a set of multiwire proportional and drift chambers and a two-plane scintillation hodoscope, the counters of which were used to measure the energy losses required for particle identification [10].

The biggest challenge that has to be faced when measuring the absolute value of a cross section in a storage ring experiment is to establish the beam-target luminosity at the few percent level even though the overlap of the beam and target cannot be deduced with such precision from macroscopic measurements. It has been shown that this can be achieved by studying the energy loss through electromagnetic processes as the coasting uncooled beam passes repeatedly through the target chamber. There is a resulting change in the frequency of the machine that can be determined with high accuracy by studying the Schottky power spectrum of the beam [11]. The amount of electromagnetic interaction is proportional to that of the strong proton–proton scattering, whose measurement was the goal of the experiment

The statistical distribution of particles in the beam is at the origin of the Schottky noise. This gives rise to current fluctuations that induce a voltage signal at a beam pick-up. The Fourier analysis of the voltage signal, i.e., of the random current fluctuations, by a spectrum analyser delivers power distributions around the harmonics of the revolution frequency. Over a 300 s cycle, the Schottky signals were recorded every 10 s with a 189 ms sweep time, thus giving effectively instantaneous spectra. The frequencies were measured with the existing Schottky pick-up of the stochastic cooling, which is optimized to operate in GHz region [12]. The harmonic number 1000 of COSY revolution frequency was measured with a more precise analyser than the one used in our previous work [11].

Some examples of these measurements scaled to harmonic number 1 are shown in Fig. 1 for circulating proton beam energies of 1.0 and 2.0 GeV. After subtracting the background noise, the mean frequency f of the beam at each instant of time was evaluated from the centroid of the distribution. Such values, which are indicated by the vertical lines, allow f to be determined as a function of time t over the 300 s cycle.

The important point to notice in Fig. 1 is that the direction of the frequency change is different at low and high energies; the energy of this transition from one regime to the other depends upon the lattice settings of the accelerator [11]. Since the luminosity is proportional to $\mathrm{d}f/\mathrm{d}t$, it means that there is a range of beam energies where the fractional errors are so large as to make the Schottky method of little practical use. This explains the gap in our data from 1.0 GeV to 1.6 GeV.

It was shown in Ref. [11] that the effective number of target particles per unit area, n_T, that interact with the proton beam is given by

$$n_T = \left(\frac{1+\gamma}{\gamma}\right)\frac{1}{\eta}\,\frac{1}{(\mathrm{d}E/\mathrm{d}x)m}\,\frac{T_p}{f^2}\,\frac{\mathrm{d}f}{\mathrm{d}t}, \qquad (1)$$

where m is the proton mass. The cluster-jet target [13] used in this experiment was very thin and, as a result, the energy changes over a 300 s cycle were extremely small ($\Delta E/E \approx 2-4\times10^{-4}$). Under such conditions one can take f and T_p to be the initial values of

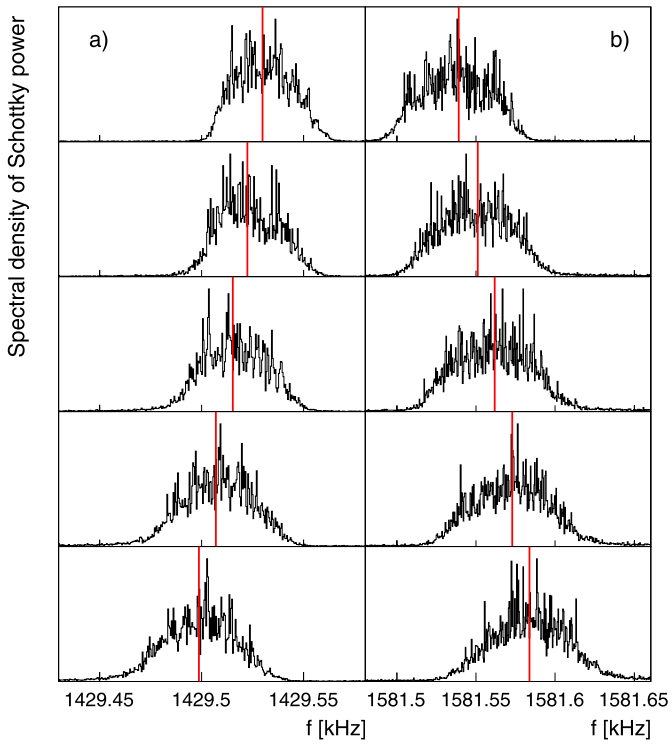

Fig. 1. Schottky power spectra obtained during one 300 s cycle and scaled to harmonic number 1 for (a) 1.0 and (b) 2.0 GeV beam energies. Although the data were recorded every 10 seconds, for ease of presentation, only the results from every 60 s are shown, starting from top to bottom. The mean frequencies are indicated by the vertical (red) lines.

the frequency and kinetic energy of the beam and γ as the corresponding Lorentz factor. The value of the stopping power $\mathrm{d}E/\mathrm{d}x$ at a given energy is to be found in the NIST–PML database [14]. The remaining quantity in Eq. (1), the so-called frequency-slip parameter η, shows how the beam revolution frequency changes with momentum. Under COSY conditions this parameter changes sign at $T_p \approx 1.3$ GeV.

Although the value of η can be estimated semi-quantitatively by a computer simulation of the acceleration process, greater precision is achieved by a direct measurement, where the change in the revolution frequency induced by adjusting the strength in the bending magnets by few parts per thousand is studied [11]. This was investigated in separate runs at each of the beam energies with the target switched off [6].

A small frequency shift is also produced by the interaction of the beam with the residual gas in the COSY ring and this was measured using dedicated cycles, where the ANKE cluster target was switched on but the beam was steered away from it. This precaution was necessary because the target produces additional background in the vicinity of the ANKE target chamber [11].

The measurement of the beam intensity, n_B, is a routine procedure for any accelerator and is performed at COSY using the high precision Beam Current Transformer device. These measurements were carried out every second over the 300 s cycle and then averaged. The final results are accurate to better than 10^{-3} [11]. The luminosity in the experiment is then the product of beam and target factors, $L = n_B n_T$.

The Forward Detector was the subject of a very detailed study [15] and only some of the salient points are mentioned here. The setup parameters were adjusted in a geometry tuning procedure, with the use of the exclusive $pp \to pp$, $pp \to pn\pi^+$, $pp \to pp\pi^0$, and $pp \to d\pi^+$ reactions. In the last case, both the d

Table 1
Systematic uncertainties in the normalisation and reconstruction procedure at different proton beam energies T_p. E_1 reflects the statistical and systematic effects in the determination of the frequency-slip parameter η. E_2 arises from the rest gas effect (including direct measurement errors as well as possible instabilities). E_3 is a measure of the density instability through the 300 s cycle. E_4 corresponds to the accuracy of the stopping powers given in the NIST database [14]. E_5 is an estimate of the precision of the analysis of data taken with the FD, including the reconstruction uncertainties. These contributions have been added in quadrature to give the total percentage uncertainty in the last column.

T_p GeV	E_1 %	E_2 %	E_3 %	E_4 %	E_5 %	Total %
1.0	1.6	0.7	0.7	1.5	1.5	2.8
1.6	1.2	1.9	1.4	1.5	1.5	3.4
1.8	1.3	1.6	1.6	1.5	1.5	3.4
2.0	0.8	1.9	1.8	1.5	1.5	3.5
2.2	0.3	1.0	1.0	1.5	1.5	2.6
2.4	0.4	1.5	1.6	1.5	1.5	3.1
2.6	0.4	1.5	1.5	1.5	1.5	3.0
2.8	0.9	1.2	0.5	1.5	1.5	2.6

and π^+ were detected in the FD and this gave valuable information on the systematics of the transverse momentum reconstruction. These showed that any systematic shift in the determination of the c.m. angle in pp elastic scattering was less than 0.15°, which would correspond to a 0.5% change in the differential cross section.

The pp elastic scattering events were detected by measuring a single proton in the FD. The trigger for the data acquisition system was initiated by a signal produced by the proton in either of the two hodoscope walls, placed one behind the other. This, together with a high scintillation counter efficiency, reduced the trigger inefficiency to the 10^{-4} level. The efficiency of each of the MWPC's planes exceeds 97%. A redundancy of the track hits allowed us to omit some of the planes in the reconstruction procedure, which led to an overall tracking efficiency of 99.5%. The acceptance was obtained in a GEANT-based simulation, taking into account the detector geometry, as well as the particle interaction with the detector material. In order to study the systematic effects, different acceptance cuts were applied in the cross section evaluation as well as different sets of wire planes used for track reconstruction. The resulting values of the cross sections showed an RMS variation of less than 1%.

The pp elastic scattering reaction produced a prominent peak in the missing-mass spectrum, with a background of only $1-2$%, and an estimated uncertainty of this level of 0.5%. A small contribution from the $pp \to d\pi^+$ reaction to the peak region at 1 GeV was subtracted on the basis of the energy-loss information. A kinematic fitting procedure, constraining the missing mass to be that of the proton, was applied to events in the pp elastic scattering peak; this reduced the systematic uncertainty of the reconstructed scattering angle, leading to an accuracy $\sigma(\theta_{\rm cm}) = 0.1°$ [15].

Table 1 lists five identified contributions to the overall systematic uncertainty of the pp elastic scattering data at the eight energies studied. No single contribution is dominant, which means that it would be hard to reduce the systematic error to much below the 2.5–3.5% total uncertainty quoted in the table. Any angular dependence in the total systematic uncertainty is smaller than the statistical errors.

The variation of the ANKE data over the ranges in angle and energy studied can be seen most clearly in the differential cross section with respect to the four-momentum transfer t and these results are shown in Fig. 2. Also shown are exponential fits to the measured data made on the basis of

$$\frac{d\sigma}{dt} = A \exp\left(-B|t| + C|t|^2\right), \qquad (2)$$

where the values of the resulting parameters are given in Table 2. Taking $C = 0$ at 1 GeV would change the value of A found in the fit by less than 1%, though this parameter becomes more important at higher energies where the t range is larger. This empirical representation of the measured data may prove helpful when the results are used in the normalisation of other experimental measurements.

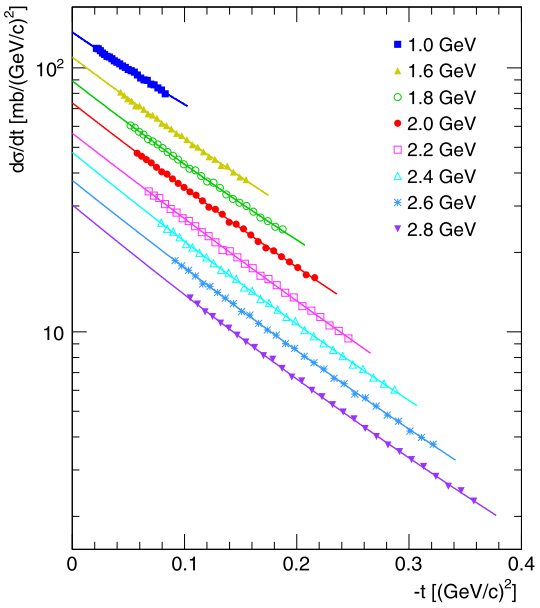

Fig. 2. Combined ANKE data set of differential cross sections with respect to the four-momentum transfer t compared to fits made on the basis of Eq. (2). Systematic errors are not shown and the statistical errors are smaller than the sizes of the symbols. The correct values are shown at 1.0 GeV but, for clarity of presentation, the other data are scaled down sequentially in energy by factors of 1.2. The true numerical values of the parameters are given in Table 2.

Table 2
Parameters of the fits of Eq. (2) to the differential cross sections measured in this experiment. In addition to the statistical errors shown, the second uncertainty in the value of A in the second column represents the combined systematic effects summarised in Table 1. The values of the parameters B and C are independent of the overall normalisation. The corrected values of the forward cross section, A(Corr.), were obtained using the SAID fit discussed in the text, the associated error bars being purely the systematic ones listed in Table 1. These values, which were not subjected to the SAID normalisation factors applied in Fig. 5, may be compared with those of A(GK), which were determined using the Grein and Kroll forward amplitudes [16] and which are shown as a smooth curve in Fig. 6.

T_p GeV	A $\frac{\rm mb}{({\rm GeV}/c)^2}$	B $({\rm GeV}/c)^{-2}$	C $({\rm GeV}/c)^{-4}$	A(Corr.) $\frac{\rm mb}{({\rm GeV}/c)^2}$	A(GK) $\frac{\rm mb}{({\rm GeV}/c)^2}$
1.0	$136.4 \pm 1.3 \pm 3.8$	6.7 ± 0.4	4.0 ± 3.8	136.7 ± 3.8	135.2
1.6	$131.7 \pm 1.9 \pm 4.5$	7.4 ± 0.3	2.7 ± 1.7	131.1 ± 4.5	128.9
1.8	$128.6 \pm 1.7 \pm 4.4$	7.6 ± 0.2	3.4 ± 1.0	127.6 ± 4.3	125.7
2.0	$127.3 \pm 1.7 \pm 4.5$	7.7 ± 0.2	2.5 ± 0.8	124.0 ± 4.3	123.1
2.2	$117.2 \pm 1.8 \pm 3.0$	7.6 ± 0.2	1.4 ± 0.7	113.1 ± 2.9	120.9
2.4	$119.2 \pm 1.8 \pm 3.7$	8.0 ± 0.2	2.7 ± 0.5	112.8 ± 3.5	118.5
2.6	$111.9 \pm 1.7 \pm 3.4$	7.8 ± 0.2	2.0 ± 0.4	108.8 ± 3.3	116.0
2.8	$108.5 \pm 1.8 \pm 2.8$	8.1 ± 0.2	2.4 ± 0.4	105.0 ± 2.7	113.6

There are very few data sets of absolute cross sections at small angles to which the ANKE results can be compared. In the vicinity of 1 GeV there are two measurements by the Gatchina group that were made with the IKAR recoil detector. In the first of these at 992 MeV, IKAR used a hydrogen target [17]. In the second at 991 MeV a methane target was used [18], though the prime purpose of this experiment was to show that such a target gave consistent results and so could be used with a neutron beam [19]. The ratio of the IKAR hydrogen values [17] to the fit of the ANKE 1000 MeV data over the common range of angles is 0.920 ± 0.005 and, in order to compare the shapes of the data sets, these IKAR

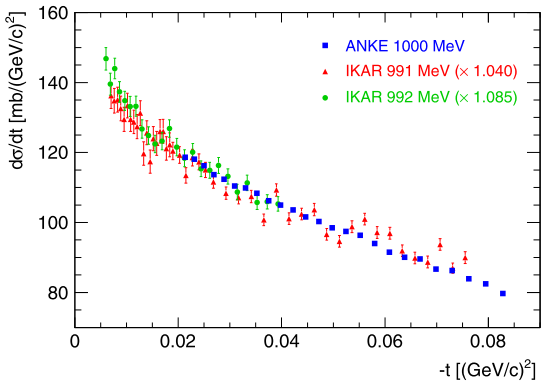

Fig. 3. Invariant differential cross section for *pp* elastic scattering. The ANKE data at 1000 MeV with statistical errors (blue squares) are compared to the IKAR hydrogen data at 992 MeV (green circles) [17] scaled by a factor of 1.085 and methane results at 991 MeV (red triangles) [18] scaled by a factor of 1.04. At very small values of $|t|$ there is a rise caused mainly by Coulomb-nuclear interference.

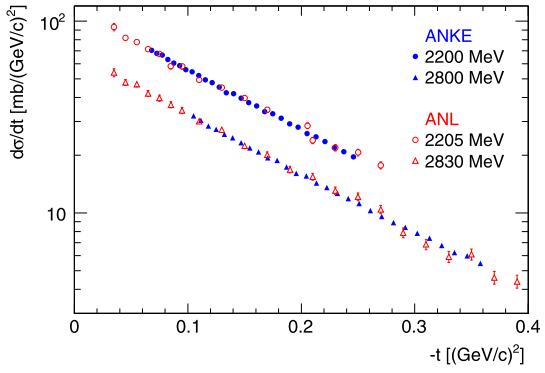

Fig. 4. The ANKE *pp* differential cross section data at kinetic energies of 2.2 GeV (closed blue circles) and 2.8 GeV (closed blue triangles) compared to the ANL results [20] at 2.2 GeV (open red circles) and 2.83 GeV (open red triangles). Only statistical errors are shown, though these are generally smaller than the sizes of the symbols. For presentational purposes, both higher energy data sets have been scaled downwards by a common factor of 1.5.

results have been scaled by a factor of 1.085 before being plotted in Fig. 3. The scaling factor is significant in view of the 2% and 2.8% absolute normalisations reported for the IKAR and ANKE experiments, respectively.

Data are also available from the Argonne National Laboratory in our angular range at kinetic energies of 2.2 and 2.83 GeV [20] and these values are plotted together with our measurements in Fig. 4. The ANL data sets agree with our 2.2 and 2.8 GeV results to within 1%. However, the absolute normalisation claimed for these data was 4% [20] so that it is not possible to draw completely firm conclusions from this comparison.

The results reported in this letter could clearly have an impact on the current partial wave solutions. This is demonstrated in Fig. 5, where the ANKE cross sections at 1.0, 2.0, and 2.8 GeV are compared to both the SAID SP07 solution [4] and a modified one that takes the present data at all eight energies into account. Scaling factors in the partial wave analysis, consistent with the overall uncertainties given in Table 1, have been included in the figure. The major changes introduced by the new partial wave solution are in the $^1S_0$ and $^1D_2$ waves at high energy. It should be noted that the modified solution does not weaken the description of the ANKE proton analysing powers presented in Ref. [5].

The precise EDDA measurements were undertaken for c.m. angles of 35° and above whereas the ANKE data finish well below this and the gap looks even bigger in terms of the momentum-

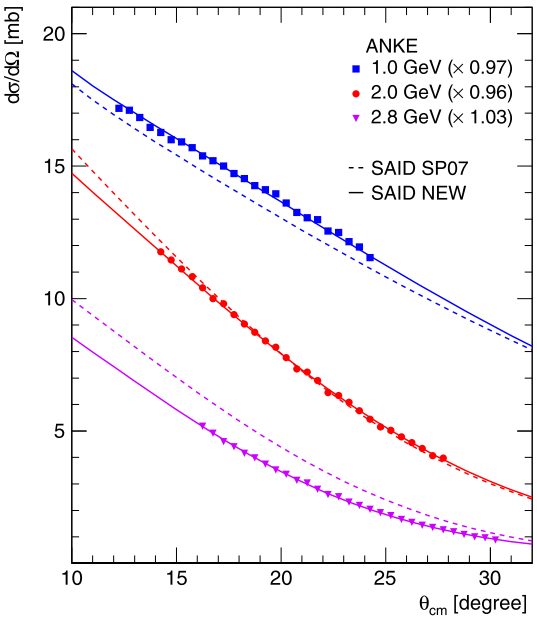

Fig. 5. Scaled ANKE proton–proton elastic differential cross sections at 1.0, 2.0, and 2.8 GeV, where the statistical errors are smaller than the sizes of the symbols. The results are compared to the SAID SP07 solution [4] (dashed line) and a modified ("new") partial wave solution (solid line) where the ANKE data have been taken into account. For presentational reasons the 2.0 and 2.8 GeV data and curves have been reduced by factors of 0.5 and 0.25, respectively. The best agreement with the new partial wave data was achieved by scaling the ANKE data with factors 0.97, 0.96, and 1.03 at the three energies. Such factors are within the uncertainties given in Table 1.

transfer variable t. Nevertheless, the modified SAID solution shown in Fig. 5 fits the ANKE 1000 MeV cross section when reduced by 3%. This solution also describes the EDDA data at 1014.4 MeV [2]. Such a 3% reduction in the ANKE normalisation at this energy is consistent with the results of a combined fit of Eq. (2) to the EDDA and the ANKE data, Coulomb-corrected as described below.

In the forward direction the number of proton–proton elastic scattering amplitudes reduces from five to three and the imaginary parts of these amplitudes are determined completely by the spin-averaged and spin-dependent total cross sections with the help of the generalised optical theorem. The corresponding real parts have been estimated from forward dispersion relations, where these total cross sections provide the necessary input [16]. All the terms contribute positively to the value of A and, using the optical theorem, the lower bound,

$$A \geq (\sigma_{\mathrm{tot}})^2/16\pi\hbar^2, \tag{3}$$

is obtained by taking the *pp* spin-averaged total cross section σ_{tot}. This lower bound and the full Grein and Kroll estimates A(GK) [16] are both shown in Fig. 6 where, for consistency, the same values of σ_{tot} were used in the two calculations.

The 992 MeV IKAR data of Fig. 3 show a significant rise at small $|t|$ that is a reflection of Coulomb distortion of the strong interaction cross section and this was taken into account through the introduction of explicit corrections [17]. The corrected data were then extrapolated to the forward direction ($t = 0$), using a simple exponential function, which would correspond to Eq. (2) with $C = 0$. The resulting points at all the energies studied are generally about 10% below the Grein and Kroll predictions and would therefore correspond to smaller real parts of the spin-dependent amplitudes. The extrapolation does, of course, depend upon the Coulomb-corrected data following the exponential fit down to $t = 0$.

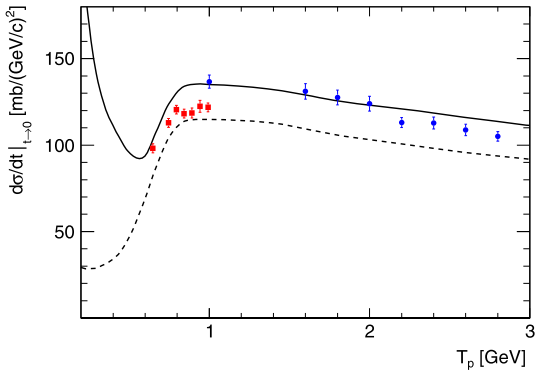

Fig. 6. The predictions of Grein and Kroll [16] for the values of the forward pp elastic differential cross section A(GK) (solid line), the corresponding lower limit provided by the spin-independent optical theorem of Eq. (3) being indicated by the broken line. The extrapolated ANKE data, corresponding to the A(Corr.) parameter of Table 2, are shown with their quoted errors by the (blue) circles, whereas the (red) squares are the published IKAR values [17].

Though the ANKE data do not probe such small $|t|$ values as those of IKAR [17], and are therefore less sensitive to Coulomb distortions, these effects cannot be neglected since they contribute between about 1.5% and 4.5% at 1.0 GeV though less at higher energies. It is seen in Fig. 5 that modified SAID solutions describe well the ANKE measurements at three typical energies and the same is true also at the energies not shown. After fitting the ANKE measurements, there is a facility in the SAID program for switching off the Coulomb interaction without adjusting the partial wave amplitudes [4] and this allows a robust extrapolation of the Coulomb-free cross section to the forward direction. The approach has the advantage that it includes some of the minor Coulomb effects that are contained in the SAID program [21,22]. It takes into account the phase variations present in the partial wave analysis and also the deviations from exponential behaviour for very small momentum transfers, $|t| \lesssim m_{\pi^0}^2 = 0.018$ (GeV/c)^2, that are linked to pion exchange. The values for A(Corr.) at $t = 0$ produced in this way are given in Table 2 and shown in Fig. 6. The error bars are purely the systematic uncertainties listed in Table 1 and any errors in the angular dependence of the SAID predictions are neglected.

The corrections obtained using the SAID program with and without the Coulomb interaction at 1 GeV are a little larger than those found by the IKAR group using an explicit Coulomb formula [17], in part due to the different relative real parts of the pp amplitude in the two calculations.

The agreement of the ANKE data with the theoretical curve in Fig. 6 is encouraging and would be even slightly better if the normalisation factors found in the fits to the cross sections in Fig. 5 were implemented. Nevertheless, the extrapolated values generally fall a little below the predictions at the higher energies.

In summary we have measured the differential cross sections for proton–proton elastic scattering at eight energies between 1.0 and 2.8 GeV in a c.m. angular domain between about 12°–16° to 25°–30°, depending on the energy. Absolute normalisation of typically 3% were achieved by measuring the energy loss of the beam as it traversed the target. After taking the Coulomb distortions into account, the extrapolations to the forward direction, are broadly compatible with the predictions of forward dispersion relations.

Although our results are completely consistent with ANL measurements at 2.2 and 2.83 GeV [20], the published IKAR values [17] are lower than ours at 1 GeV by about 8%, though this would be reduced to about 5% if one accepts the renormalisation factor from the SAID fit shown in Fig. 5.

The new ANKE data have a significant influence on a partial wave analysis of this reaction, as illustrated at three energies in Fig. 5. In the revised solution, the $^1S_0$ and $^1D_2$ waves in particular change at high energies and this will be made clearer in an update to the SAID SP07 solution [4]. On a more practical level, the measurements will also be a valuable tool in the normalisation of other experiments.

We acknowledge valuable discussions with Peter Kroll, who provided the numerical values of the predictions shown in Ref. [16]. We also are grateful to other members of the ANKE Collaboration for their help with this experiment and to the COSY crew for providing such good working conditions. This material is based upon work supported by the Forschungszentrum Jülich (COSY-FEE), the Shota Rustaveli Science Foundation Grant (#31/91), and the U.S. Department of Energy, Office of Science, Office of Nuclear Physics, under Award Number DE-FG02-99-ER41110.

References

[1] D. Albers, et al., Phys. Rev. Lett. 78 (1997) 1652.
[2] D. Albers, et al., Eur. Phys. J. A 22 (2004) 125.
[3] M. Altmeier, et al., Eur. Phys. J. A 23 (2005) 351.
[4] R.A. Arndt, I.I. Strakovsky, R.L. Workman, Phys. Rev. C 62 (2000) 034005; R.A. Arndt, W.J. Briscoe, I.I. Strakovsky, R.L. Workman, Phys. Rev. C 76 (2007) 025209, http://gwdac.phys.gwu.edu.
[5] Z. Bagdasarian, et al., Phys. Lett. B 739 (2014) 152.
[6] D. Chiladze, in: Proc. 8th Int. Conf. Nucl. Phys. at Storage Rings, PoS (STORI11) 039, 2011.
[7] A.J. Simon, et al., Phys. Rev. C 48 (1993) 662.
[8] S. Barsov, et al., Nucl. Instrum. Methods, Sect. A 462 (2001) 364.
[9] R. Maier, et al., Nucl. Instrum. Methods, Sect. A 390 (1997) 1.
[10] S. Dymov, et al., Part. Nucl. Lett. 2 (119) (2004) 40.
[11] H.J. Stein, et al., Phys. Rev. Spec. Top., Accel. Beams 11 (2008) 052801.
[12] D. Prasuhn, et al., Nucl. Instrum. Methods Phys. Res., Sect. A 441 (2000) 167.
[13] A. Khoukaz, et al., Eur. Phys. J. D 5 (1999) 275.
[14] NIST–PML database, http://www.nist.gov/pml/data/star.
[15] S. Dymov, ANKE internal report #32, available from http://collaborations.fz-juelich.de/ikp/anke/internal.shtml.
[16] W. Grein, P. Kroll, Nucl. Phys. A 377 (1982) 505.
[17] A.V. Dobrovolsky, et al., Nucl. Phys. B 214 (1983) 1.
[18] A.V. Dobrovolsky, et al., report LNPI-1454, 1988.
[19] B.H. Silverman, et al., Nucl. Phys. A 499 (1989) 763.
[20] I. Ambats, et al., Phys. Rev. D 9 (1974) 1179.
[21] R.A. Arndt, et al., Phys. Rev. D 28 (1983) 97.
[22] C. Lechanoine, F. Lehar, F. Perrot, P. Winternitz, Nuovo Cimento A 56 (1980) 201.